Frontiers in Health Informatics
ISSN-Online: 2676-7104
www.healthinformaticsjournal.com
2024; Vol 13: Issue 2
Open Access

Harnessing ResNet50 and DenseNet201 for Enhanced Lymphoma Diagnosis via Feature Extraction

Mrs.Deepthi.S[1], DR.Malepati Chandra Sekhar[2]

[1]Assistant Professor, School of Computer Science and Engineering, Presidency University, Bengaluru, India.

[2]Professor, School of Computer Science and Engineering, Presidency University, Bengaluru, India.

Article Info

Article type:
Research

Article History:
Received: 2024-03-30
Revised: 2024-05-29
Accepted: 2024-06-26

Keywords:
Accuracy, DenseNet201, feature extraction, lymphoma, pre-trained convolutional neural networks, ResNet50.

A B S T R A C T

Introduction: A form of malignant tumour known as lymphoma originated in lymphoid hematopoietic organs. Because the physical characteristics of the many lymphoma classes are similar, accurately diagnosing lymphomas is one of the most difficult tasks. Hence, an efficient classification of lymphoma plays a very important role in order to provide patients with prompt care. The purpose of this work is to evaluate the performance of pre-trained Convolutional Neural Networks (CNNs) in the multiclass categorization of lymphomas.

Objectives: Classification of Non-Hodgkin lymphomas by adopting pre-trained CNN architectures like ResNet50, VGG16, InceptionV3 and DenseNet201 are adopted. Utilize several pre-processing techniques for denoising, rescaling, and enriching the input images, including gaussian filter, min-max normalisation, and data augmentation. Perform a detailed performance analysis of the proposed work with existing models.

Methods: This research uses the different CNN architectures such as VGG16, DenseNet201, InceptionV3 to classify the lymphoma. In pre-processing, the gaussian filter is used to denoise and smoothen the images, min-max normalization is used to rescale the images and the data augmentation is used for solving the data imbalance issue. Transfer Learning and Fine-Tuning is done which improves the overall performance of the model.

Results: This study makes use of the multi cancer dataset from Kaggle. The performance of these pre-trained CNN models is evaluated using accuracy, precision, recall, and the F-measure. Based on simulation findings, DenseNet201 outperforms VGG16 and InceptionV3 with an accuracy of 99.90%. Furthermore, FFNN-ResNet50 and HPC are two current studies that are used to compare ResNet50 and DenseNet201. ResNet50-DenseNet201 has a high accuracy of 99.90% compared to FFNN-ResNet50 and HPC.

Conclusions: Several CNN architectures, including VGG16, InceptionV3 and DenseNet201 are employed in this study to categorize lymphomas. Several NHL classifications, including FL, CLL, and MCL, are classified using the pre-trained CNN architecture. The gaussian filter, which aids in smoothing the pictures, is used to eliminate noise from the histopathology images. The pixel limits are then scaled using min-max normalization to increase pixel intensity, and data augmentation is employed to prevent data imbalance problems. Improved categorization is achieved by the ResNet50 by extracting multi-scale characteristics from the images. Based on the simulation findings, it is evident that DenseNet201, which incorporates ResNet50 features, outperforms VGG16 and InceptionV3 due to the intricate interactions between data that dense connectivity enables. Furthermore, ResNet50-DenseNet201 performs better than FFNN-ResNet50 and HPC. In comparison to FFNN-ResNet50 and HPC, ResNet50-DenseNet201 has a high accuracy of 99.90%.

INTRODUCTION

The term Non-Hodgkin lymphoma (NHL) refers to a broad category of lymphoid cancers that originate from natural killer cells, T cells, or B cells. It is distinguished by a range of genetic anomalies, different histopathological characteristics with heterogeneous clinical traits. Precise NHL subtype identification is essential for patient management, therapy planning, and prognosis. Conventional approaches to NHL categorization mainly depend on immunophenotyping, genetic profiling, and histopathological analysis. Although these techniques are useful, they are time-consuming, subjective, and may be vulnerable to inter-observer variability. The application of deep learning and other advanced machine learning approaches to automate and improve NHL categorization accuracy has garnered increasing attention in recent years.

This is the third most common cancer in children and the most common hematologic malignancy [1] [2]. The epidemiological characteristics of lymphoma, such as the proportion, age of onset, and sex ratio, vary according to racial, social, and environmental factors [3]. Hodgkin lymphoma (HL) and non-Hodgkin lymphoma (NHL) are the two main categories for lymphoma [4]. While reactive hyperplasia, inflammation, and TB are caused by benign lesions, lymphomas and metastases are significant malignant lesions [5]. NHL is a cancer of the lymphoid system that commonly extends to distant organs [7]. The primary classifications of NHL are Follicular Lymphoma (FL), Mantle Cell Lymphoma (MCL), and Chronic Lymphocytic Leukemia (CLL) [8]. NHL is a broad term for malignant tumors with a fast pace of growth.There are approximately 70 subclasses of malignant lymphomas, and pathologists identify the subclass based on a set of invasively collected microscopic pictures from the patient in order to choose the best course of treatment [12]. Typically, the tissue stained with hematoxylin-eosin (H&E) is used by pathologists to identify lymphomas. When attempting to classify the type of lymphoma, this procedure is challenging and time-consuming [13].
Somaratne, U.V et al. [16] presented the Generative Adversarial Networks (GAN) for generating the synthetic Whole Slide Image (WSI) patches. The distinction between target and non-target WSI patches was made using CNN. The created CNN could only classify the FL; multiclass classification was necessary for an accurate diagnosis.

Ammar Ammar et.al. [17] used InceptionResNetV2 model. The method works by splitting the images into patches, classifying each patch using a deep learning model and achieved 87.0% three-class classification accuracy.

The transfer learning was presented by Soltane, S. et al. [18] to help pathologists classify lymphomas. Here, transfer learning was used to create the Residual Neural Networks and ResNet50 for the purpose of identifying and classifying the lymphoma. However, a large number of images needed for these transfer learning techniques to boost categorization abilities farther.

Two distinct methods were used by Al-Mekhlafi, Z.G. et al. [19] for the histology images, DenseNet-121 and ResNet-50. Additionally, the Feed-Forward Neural Network (FFNN) classifier was used to complete the classification. The combination of FFNN, along with ResNet-50 and Densenet201 produced better classification results.

The new method [20] presented by Somaratne, U.V., Wong, K.W., Parry, J. et al. minimizes the requirement for tagged data while handling interstice differences. In order to reduce the number of labels needed and enhance efficacy, a GAN-based approach has been presented to solve the one-class data problem. The research demonstrates that, when applied to the data from the new site, the suggested GAN-based method performs noticeably better. It is possible to improve the suggested method while using less computer power.

The Fractal Neural Network (FNN), which uses CNN and fractal geometry to identify histology pictures, was introduced by Roberto, G.F. et al. [21]. The fractal characteristics were extracted from the histology pictures and rearranged to create the artificial RGB feature image. Next, the input and its pertinent fake picture were used to classify the CNN ensemble. An image's qualities can be described by integrating different fractal metrics to provide a set of features. In order to improve the categorization even further, the constructed FNN has to take the deep features into account.

The Faster Region-Convolutional Neural Network (Faster R-CNN) was created by Sheng, B. et al. [22] in order to classify lymphoma cells. Along with the lymphocyte cells, color images of blast cells were added to assess the Faster R-CNN's robustness and dependability. To effectively classify lymphomas, the subclasses of the disease had to be taken into account.

OBJECTIVES

a) Classification of Non-Hodgkin lymphomas by adopting pre-trained CNN architectures like ResNet50, VGG16, InceptionV3 and DenseNet201. 2)Utilize several pre-processing techniques for denoising, rescaling, and enriching the input images, including gaussian filter, min-max normalisation, and

data augmentation. C)Study a detailed performance analysis of the proposed work with existing models like FFNN-ResNet50 and HPC.

METHODS

This study analyses the Non-Hodgkin lymphoma classification using a variety of pre-trained CNNs, including ResNet50, InceptionV3, VGG16, DenseNet201. This study examines four distinct processes: 1) acquiring the dataset; 2) pre-processing; 3) extracting features; and 4) classification. The ResNet50 extracts the features from the pre-processed images which used to discard the issue of vanishing gradient is illustrated in the Figure 1.

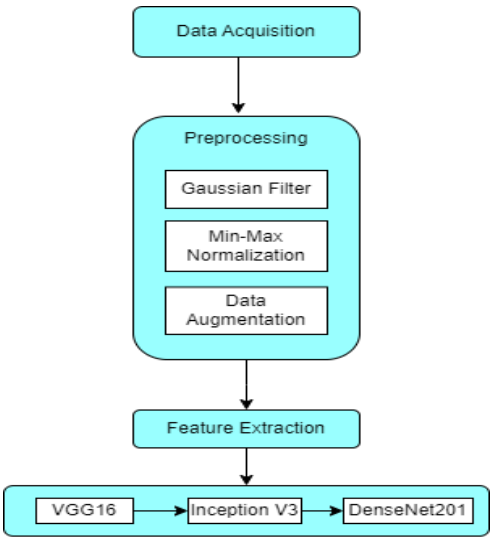

Fig 1. Block diagram of CNN models for the classification of Lymphoma

Dataset acquisition

This study makes use of the Multi cancer dataset from Kaggle to investigate the histopathology images. There are fifteen thousand photos in the Multi Cancer dataset, which is divided into three classes: FL, CLL, and MCL. The JPEG format is used to save the 512x512 photos that make up the collection.

Data pre-processing

The images from the dataset are preprocessed using Gaussian filter, min-max normalization and data augmentation processes.

In image processing, Gaussian filters are frequently used to reduce noise in image while keeping crucial details. A Gaussian function is used to convolve the image in order to apply Gaussian filters. This function emphasizes pixels closer to the center of the kernel more than those at its edges. This results in a smoothing effect that reduces high-frequency noise, like salt-and-pepper noise or Gaussian noise, while preserving the image's edges and clarity.

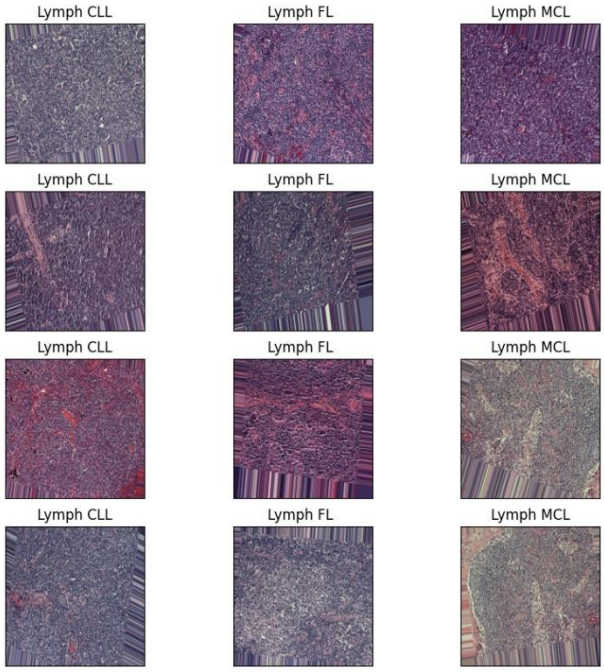

Fig 2. Sample images from the dataset

Gaussian filter of the pixel (i, j) uses 2 dimensional Gaussian distribution as shown in equation (1).

$$G(i,j) = \frac{1}{2\pi\sigma^2} e^{\frac{-i^2+j^2}{2\sigma^2}} \quad (1)$$

Where, standard deviation is denoted as σ and the filtered image is denoted as G.Min-Max normalization is a quick and efficient method for rescaling pixel values to a desired range in image preprocessing. It preserves the associations between pixels' relative intensities, which is essential for the clarity of the image and its visual perception. The pixel intensity of the filtered images are enhanced by scaling the pixel limits using the min-max normalization as shown in equation (2).

$$G' = (G - min)\frac{newmax - newmin}{max - min} + newmin \quad (2)$$

Where, G' is scaled output; maximum and minimum of filtered image is denoted as max and min; $newmin$ and $newmax$ are scaled image's intensity values.

Data augmentation is a preprocessing approach that applies random changes to preexisting images to artificially improve the diversity of training data. This enables deep learning models, such as ResNet50, which are prone to overfitting when trained on small amounts of data, become more resilient and more broadly applicable.

The data augmentation is done through the operations of rotation, horizontal flipping and zooming for scaled images. The preprocessed image is given as input to ResNet50 to perform feature extraction. Data augmentation helps prevent the model from memorizing specific examples and instead focuses on learning generalizable features.

Feature extraction using ResNet50

ResNet50 is a powerful image classification model that can be trained on large datasets and achieve state-of-the-art results, without having to suffer from the problem of vanishing gradients. In this phase, the pre-trained deep residual neural network i.e., ResNet50 [24] is used to extract the multi scale features.

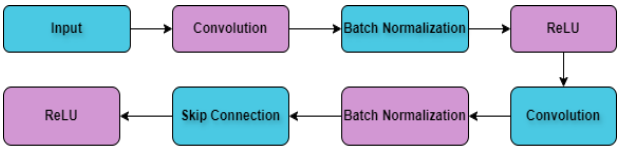

Fig 3. Step-by-Step process

Max pooling layers, which decrease the spatial dimensions of the feature maps while maintaining the most significant features, appear after the convolutional layers. ResNet facilitates the direct path between input and output by guiding the transitional weight levels, supporting the network layers for learning from the identity function. Figure 3 shows the architecture of ResNet50 based feature extraction.

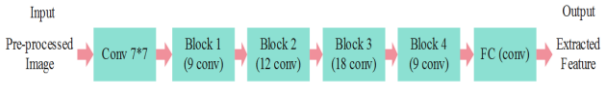

Fig 4. Architecture of ResNet50 based feature extraction

A residual block in ResNet50 consists of two main paths: the identity mapping path and the residual mapping path,therefore the final output of ResNet is expressed in equation (3).

$$y = F(x) + x \tag{3}$$

Where, x is input, y is output and residual mapping is denoted as $F(x)$.

The architecture of ResNet50 is depicted in Figure 4, and it first performs the convolutional operation on the input. There are 50 Conv2D procedures in the ResNet50 architecture. Moreover, the features of the preceding layer are summarized at the end of ResNet50 using the Fully Connected (FC) layer. Whereas the previous convolution and pooling operations are seen as the feature extraction process, the FC layer is thought of as feature weighting. The nonlinear combinations of improved attributes produced by the Conv layer can be observed by the FC layer.

Utilizing pretrained CNN models for classification

In this stage, the pre-trained CNN models such as VGG16, InceptionV3, DenseNet201 are used to analyze the multi class Lymphoma classification. The typical architecture of CNN is shown in the Figure 5.

CNN's ability to learn from its own features and its ability to classify images more accurately than other methods makes it the best choice for image-based categorization. The input, convolution, pooling, fully connected, and classification output layers are used in the design of the CNN. Convolution layer, the core layer of CNN, incorporates a small-size filters that encompasses the entire input. Completing the dot product between the input and filter guarantees the convolution process. The filter is stepped in the following position because the dot product is included through the filter.

Thus, a whole input is processed in convolution process. The convolution (z) among the filter vector and input (p) and is expressed in equation (4).

$$z_j^l = \varphi(p_j^{l-1} \times w_{ij}^{(1)l} + b_j^{(1)l}) \tag{4}$$

Where, φ denotes the sigmoid activation function; bias value of lth layer and jth node is denoted as b_j^l and weight between the node i and j is denoted as $w_{ij}^{(1)l}$. Subsequently, the pooling layer carries out the maximum pooling procedure, in which the maximum pooling filter provides the maximum value for every region. In FC, every neuron at a subsequent layer is connected to every other neuron from the layer before it. The FC process is expressed in equation (5).

$$FC_j^l = \varphi(z_j^{l-1} \times w_{ij}^{(2)l} + b_j^{(2)l}) \tag{5}$$

Where, weight and bias value of FC layer are denoted as $w_{ij}^{(2)l}$ and $b_j^{(2)l}$ respectively.

Every neuron in the FC layer is coupled to an input obtained from the preceding layer. As a result, the FC layer has a significant number of training parameters. However, generating a very modest activation is how the deep learning in the FC layer is achieved. By generating sparsity, the activity of neurons is restricted, assisting in preventing the overfitting problem in CNN. Furthermore, the softmax function is used to calculate the probability distribution of an event via several events. Using softmax, the probability of every target is calculated for every target class.

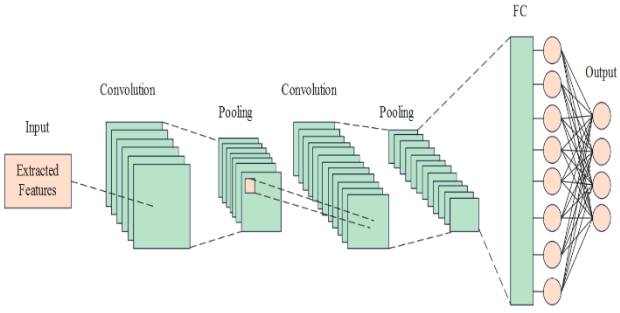

Fig 5. Architecture of CNN

The specific information about the pre-trained CNN models used in this research are detailed as follows:

VGG16

The ImageNet dataset is typically used to train the VGG-16 network. Even with minimal datasets, the VGG-16 provides higher classification because of its extensive training. This VGG-16 features a tiny 3x3 receptive field and 16 convolution (Conv) layers. It has five Max pooling layers in all, the largest of which is a 2x2 Max pooling layer. The VGG-16 employs three Fully Connected (FC) layers, with the softmax classifier serving as the last layer, following Max pooling. It also uses the ReLu activation for all hidden layers.

InceptionV3

One of the pre-trained models - Inception V3, is created using Convolution layers with various kernel sizes, pooling strategies, and dimensionality reductions. The various convolution filtering techniques utilized in the Inception V3 feature max and average pooling layers in addition to convolution sizes of 1×1, 3×3, and 5×5. Additionally, adding batch normalization and dropout improves the effectiveness of the model as well. To complete the prediction, it also uses an additional classifier and factored convolution.

DenseNet201

Several salient features set DenseNet-201 apart from other pretrained CNN models in the image classification domain. Because of its dense connectivity pattern, which guarantees that every layer receives direct inputs from every layer before it, the network is able to reuse features. In addition to improving parameter efficiency by eliminating pointless computations, this also helps to improve gradient flow during training, which solves the vanishing gradient issue that is frequently present in deeper networks. In comparison to models such as ResNet or Inception networks, DenseNet-201 is computationally lighter without compromising performance because to its compactness, which is the result of its efficient parameter usage. Furthermore, for a variety of datasets, the dense connections function as a type of implicit regularization, enhancing generalization and lowering overfitting. DenseNet-201 has proven to be a reliable performer across a range of benchmarks, frequently attaining cutting-edge outcomes in image classification assignments like ImageNet. Its proficiency in handling intricate visual identification tasks is largely attributed to its adept use of feature propagation.

RESULTS

This section contains information about the various analyses that are used to calculate the results of pre-trained CNNs. Using Anaconda Navigator, a Python programming language, a multi-class lymphoma classification is constructed. The multi-cancer dataset is used to evaluate pre-trained CNNs, while the 70:30 ratio is taken into account during the training and testing phases.This Lymphoma classification is analyzed using Accuracy, Precision, Recall and F-score which is expressed in equations (6) to (9).

$$Accuracy = \frac{TP+TN}{TN+TP+FN+FP} \times 100 \quad (6)$$

$$Precision = \frac{TP}{TP+FP} \times 100 \quad (7)$$

$$Recall = \frac{TP}{TP+FN} \times 100 \quad (8)$$

$$F-score = \frac{2Precision \times Recall}{Precision+Recall} \quad (9)$$

Where, true positive and true negative are represented as TP and TN respectively. On the other hand, false positive and false negative are represented as FP and FN respectively.

Performance analysis

This study considers three different pre-trained models such as VGG16, InceptionV3 and DenseNet201. The accuracy and loss graph for these pre-trained models are shown in the Figures 6 and 7 respectively. The AlexNet has the higher fluctuations between the training and validation accuracy whereas Densenet201 has the less fluctuations between the accuracies.

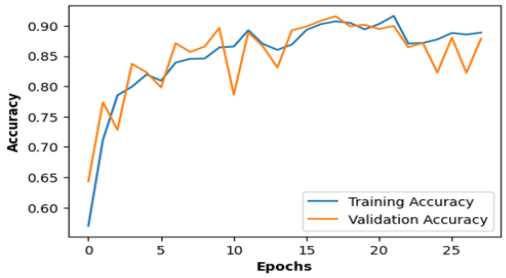

(a)

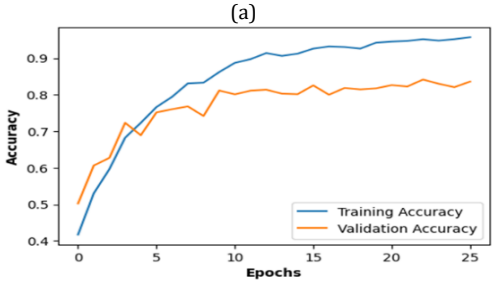

(b)

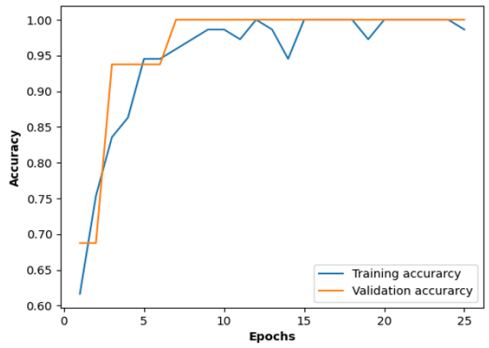

(c)

Fig 6. Training and Validation accuracy, a) VGG16, b) InceptionV3, c) DenseNet201

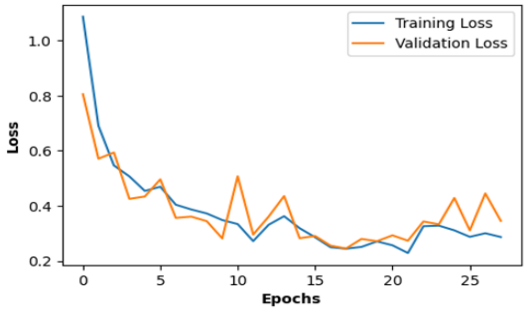

(a)

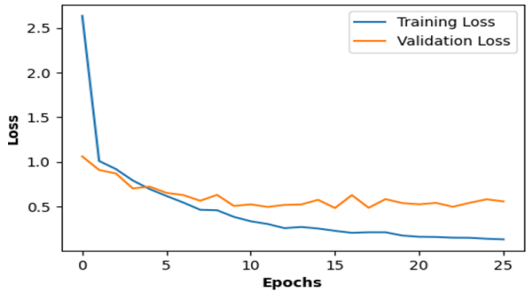

(b)

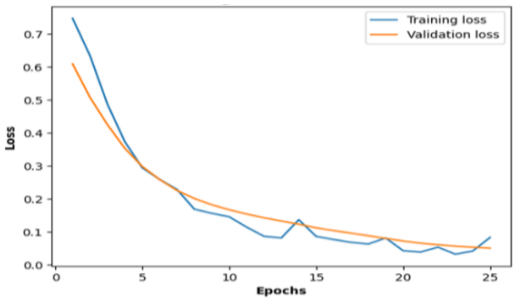

(c)

Fig 7. Training and Validation Loss, a) VGG16, b) InceptionV3, c) DenseNet201

Moreover, the performance of each pre-trained CNN for 25 epochs are shown in the Table 2. The graphical comparison of different Pre-trained CNN models is shown in the Figure 8. The outcomes depicts that classification accuracy is 90.00%, 82.56% and 99.90% for VGG16, InceptionV3 and DenseNet201 respectively. This analysis clears that DenseNet201 achieves improved classification when compared to the VGG16 and InceptionV3. DenseNet201's dense connection is utilized to extract the intricate associations in the data that enhance categorization.

Table 2. Analysis of different Pre-trained CNN models

Models	Accuracy (%)	Precision (%)	Recall (%)	F-Score (%)
VGG16	90.00	90.00	90.00	90.00
InceptionV3	82.56	84.54	82.06	83.28
DenseNet201	99.90	99.90	99.90	99.90

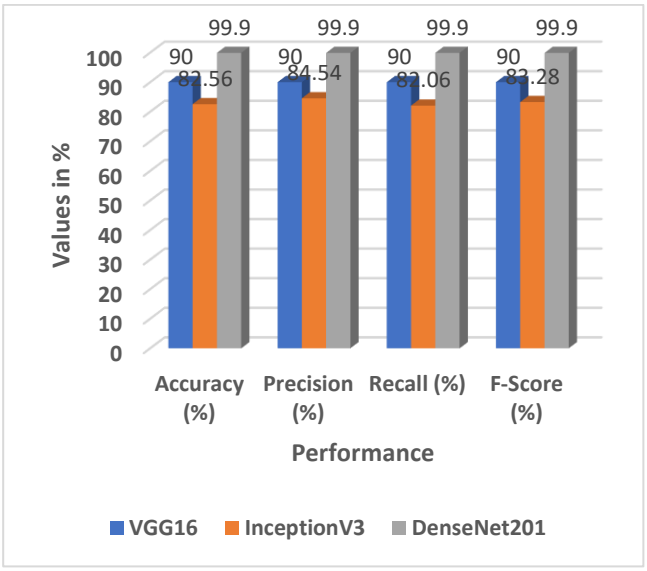

Fig 8. Graph for different Pre-trained CNN models

The confusion matrix for the Pre-trained CNN models is shown in the Figure 9.

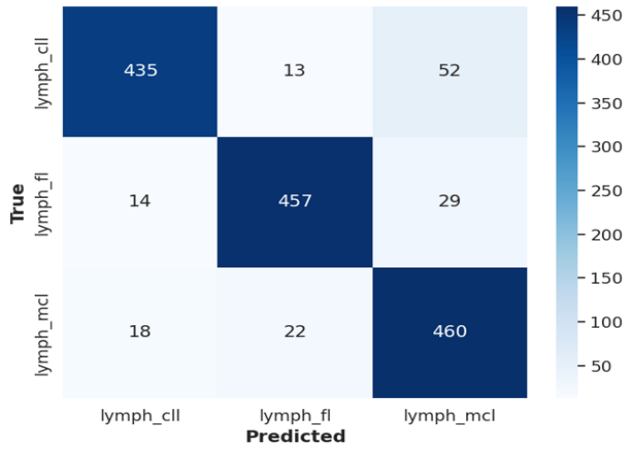

(a)

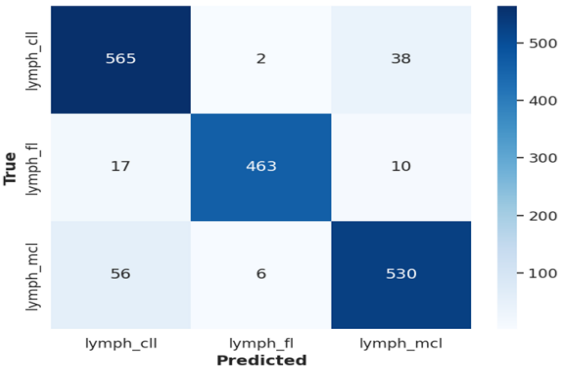

(b)

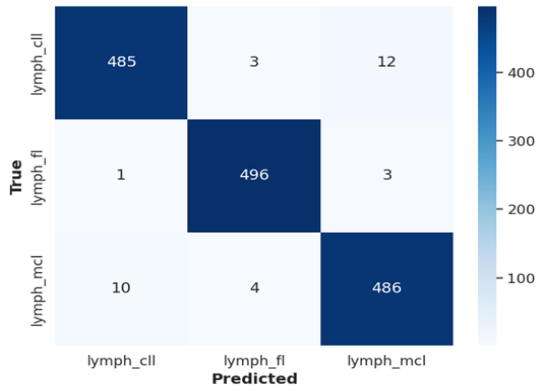

(c)

Fig 9. Confusion matrix, a) VGG16, b) InceptionV3, c)DenseNet201

Additionally, as indicated in Table 3, K-fold validation is used to examine the pre-trained CNN models. K folds 1, 3, and 5 were taken into consideration for this study. Predictive techniques are typically assessed using the K-fold validation. It is evident from the analysis that the pre-trained models performed better when the fold value was 5.

Table 3. Analysis of Pre-trained CNN models using K-fold validation

K-Fold	Classifiers	Accuracy (%)	Precision (%)	Recall (%)	F-Score (%)
K=1	VGG16	88.64	89.02	89.24	89.12
	InceptionV3	80.64	82.58	82.96	82.77
	DenseNet201	97.58	97.60	97.40	97.49
K=3	VGG16	91.33	89.84	89.48	89.66
	InceptionV3	81.42	82.84	82.62	82.73
	DenseNet201	98.88	97.80	98.28	98.04
K=5	VGG16	90.00	90.00	90.00	90.00
	InceptionV3	82.56	84.54	82.06	83.28
	DenseNet201	99.90	99.90	99.90	99.90

DISCUSSION

Comparative analysis

The existing methods such as HPC [17] and FFNN-ResNet50 [19] are used to compare the VGG16, InceptionV3 and DenseNet201. These CNN models are operated along with the ResNet50 feature extraction. The comparative analysis of ResNet50-DenseNet201 with HPC [17] and FFNN- ResNet50 [19] is shown in the Table 4. Further, the accuracy comparison is illustrated in the Figure 10. This comparison cleared that ResNet50-DenseNet201 has better classification performance than the HPC [17] and FFNN-ResNet50 [19]. The multi scale features from the ResNet50 and complex relationships among the data obtained by DenseNet201 are used to enhance the lymphoma classification.

Table 4. Comparative analysis of ResNet50-DenseNet201

Models	Accuracy (%)	Precision (%)	Recall (%)	F-Score (%)
HPC [17]	97.60	NR	NR	NR
FFNN-ResNet50 [19]	99.4	99.7	99.5	99.5
ResNet50-VGG16	90.00	90.00	90.00	90.00
ResNet50-InceptionV3	82.56	84.54	82.06	83.28
ResNet50-Densenet201	99.90	99.90	99.90	99.90

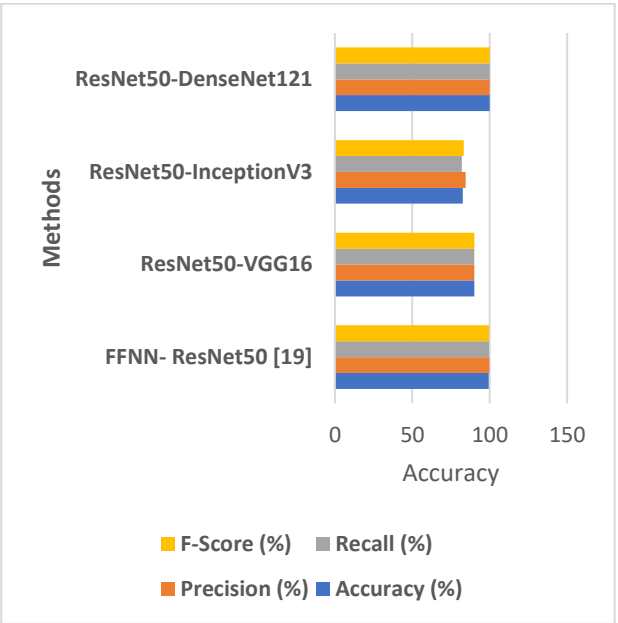

Fig 10. Accuracy comparison

CONCLUSION

Several CNN architectures, including VGG16, InceptionV3 and DenseNet201 are employed in this study to categorize lymphomas. Several NHL classifications, including FL, CLL, and MCL, are classified using the pre-trained CNN architecture. The gaussian filter, which aids in smoothing the pictures, is used to eliminate noise from the histopathology images. The pixel limits are then scaled using min-max normalization to increase pixel intensity, and data augmentation is employed to prevent data imbalance problems. Improved categorization is achieved by the ResNet50 by extracting multi-scale characteristics from the images. Based on the simulation findings, it is evident that DenseNet201, which incorporates ResNet50 features, outperforms VGG16 and InceptionV3 due to the intricate interactions between data that dense connectivity enables. Furthermore, ResNet50-DenseNet201 performs better than FFNN-ResNet50 and HPC. In comparison to FFNN-ResNet50 and HPC, ResNet50-DenseNet201 has a high accuracy of 99.90%.

AUTHOR'S CONTRIBUTION

First author contributed to the literature review, design, data collection and analysis, drafting the manuscript. Second author read and approved the final manuscript.

CONFLICTS OF INTEREST

The authors declare no conflicts of interest regarding the publication of this study.

FINANCIAL DISCLOSURE

No financial interests related to the material of this manuscript have been declared.

ETHICS APPROVAL

Not Applicable.

REFRENCES

[1] Wang, H., Liu, Z., Yang, J., Sheng, L. and Chen, D., 2023. Using Machine Learning to Expand the Ann Arbor Staging System for Hodgkin and Non-Hodgkin Lymphoma. BioMedInformatics, 3(3), pp.514-525.

[2] Tanenbaum, R.E., Galor, A., Dubovy, S.R. and Karp, C.L.,2019. Classification, diagnosis, and management of conjunctival lymphoma. Eye and Vision, 6, pp.1-16.

[3] Muto, R., Miyoshi, H., Sato, K., Furuta, T., Muta, H., Kawamoto, K., Yanagida, E., Yamada, K. and Ohshima, K., 2018. Epidemiology and secular trends of malignant lymphoma in Japan: Analysis of 9426 cases according to the World Health Organization classification. Cancer Medicine, 7(11), pp.5843-5858.

[4] Klimont, M., Oronowicz-Jaśkowiak, A., Flieger, M., Rzeszutek, J., Juszkat, R. and Jończyk-Potoczna, K., 2023. Deep Learning-Based Segmentation and Volume Calculation of Pediatric Lymphoma on Contrast-Enhanced Computed Tomographies. Journal of Personalized Medicine, 13(2), p.184.

[5] Zhang, W., Peng, J., Zhao, S., Wu, W., Yang, J., Ye, J. and Xu, S., 2022. Deep learning combined with radiomics for the classification of enlarged cervical lymph nodes. Journal of Cancer Research and Clinical Oncology, 148(10), pp.2773-2780.

[6] Frood, R., Clark, M., Burton, C., Tsoumpas, C., Frangi, A.F., Gleeson, F., Patel, C. and Scarsbrook, A., 2022. Utility of pre-treatment FDG PET/CT–derived machine learning models for outcome prediction in classical Hodgkin lymphoma. European radiology, 32(10), pp.7237-7247.

[7] Espín-Pérez, A., Brennan, K., Ediriwickrema, A.S., Gevaert, O., Lossos, I.S. and Gentles, A.J., 2022. Peripheral blood DNA methylation profiles predict future development of B-cell Non-Hodgkin Lymphoma. NPJ precision oncology, 6(1), p.53.

[8] Bai, J., Jiang, H., Li, S. and Ma, X., 2019. Nhl pathological image classification based on hierarchical local information and googlenet-based representations. BioMed research international, 2019.

[9] Carreras, J., Roncador, G. and Hamoudi, R., 2022. Artificial intelligence predicted overall survival and classified mature B-cell neoplasms based on Immuno-oncology and immune checkpoint panels. Cancers, 14(21), p.5318.

[10] Lisson, C.S., Lisson, C.G., Mezger, M.F., Wolf, D., Schmidt, S.A., Thaiss, W.M., Tausch, E., Beer, A.J., Stilgenbauer, S., Beer, M. and Goetz, M., 2022. Deep neural networks and machine learning radiomics modelling for prediction of relapse in mantle cell lymphoma. Cancers, 14(8), p.2008.

[11] Tian, R., Ma, H., Zhu, S., Lau, J., Ma, R., Liu, Y., Lin, L., Chandra, S., Wang, S., Zhu, X. and Deng, H., 2020. Multiplexed NIR-II probes for lymph node-invaded cancer detection and imaging-guided surgery. Advanced Materials, 32(11), p.1907365.

[12] Hashimoto, N., Ko, K., Yokota, T., Kohno, K., Nakaguro, M., Nakamura, S., Takeuchi, I. and Hontani, H., 2022. Subtype classification of malignant lymphoma using immunohistochemical staining pattern. International Journal of Computer Assisted Radiology and Surgery, 17(7), pp.1379-1389.

[13] Fazlali, F., Hashemi, P., Khoshfetrat, S.M., Halabian, R., Baradaran, B., Johari-Ahar, M., Karami, P., Hajian, A. and Bagheri, H., 2021. Electrochemiluminescent biosensor for ultrasensitive detection of lymphoma at the early stage using CD20 markers as B cell-specific antigens. Bioelectrochemistry, 138, p.107730.

[14] Brancati, N., De Pietro, G., Frucci, M. and Riccio, D., 2019. A deep learning approach for breast invasive ductal carcinoma detection and lymphoma multi-classification in histological images. Ieee Access, 7, pp.44709-44720.

[15] Miranda-Filho, A., Piñeros, M., Znaor, A., Marcos-Gragera, R., Steliarova-Foucher, E. and Bray, F., 2019. Global patterns and trends in the incidence of non-Hodgkin lymphoma. Cancer causes & control, 30, pp.489-499.

[16] Somaratne, U.V., Wong, K.W., Parry, J. and Laga, H., 2023. The use of generative adversarial networks for multi-site one-class follicular lymphoma classification. Neural Computing and Applications, 35(28), pp.20569-20579.

[17] A. Ammar, I. T. Kurniawan, R. N. Azizah, H. R. Yusuf, A. E. Nugroho, G. F. Mufiddin, I. Anshori, W. Adiprawita, H. A. Usman, and O. Husain, "Deep Learning for Lymphoma Detection on Microscopic Images," IEEE Transactions on Medical Imaging, vol. 42, no. 3, pp. 1123-1130, March 2025.

[18] Soltane, S., Alsharif, S. and Eldin, S.M.S., 2022. Classification and Diagnosis of Lymphoma's Histopathological Images Using Transfer Learning. Computer Systems Science & Engineering, 40(2).

[19] Al-Mekhlafi, Z.G., Senan, E.M., Mohammed, B.A., Alazmi, M., Alayba, A.M., Alreshidi, A. and Alshahrani, M., 2022. Diagnosis of histopathological images to distinguish types of malignant lymphomas using hybrid techniques based on fusion features. Electronics, 11(18), p.2865.

[20] Somaratne, U.V., Wong, K.W., Parry, J. et al. The use of generative adversarial networks for multi-site one-class follicular lymphoma classification. Neural Computing and Applications, 35(8), 1-11. https://doi.org/10.1007/s00521-023-08810-8.

[21] Roberto, G.F., Lumini, A., Neves, L.A. and do Nascimento, M.Z., 2021. Fractal neural network: A new ensemble of fractal geometry and convolutional neural networks for the classification of histology images. Expert Systems with Applications, 166, p.114103.

[22] Sheng, B., Zhou, M., Hu, M., Li, Q., Sun, L. and Wen, Y., 2020. A blood cell dataset for lymphoma classification using faster R-CNN. Biotechnology & Biotechnological Equipment, 34(1), pp.413-420.

[23] Multi cancer dataset: https://www.kaggle.com/datasets/obulisainaren/multi-cancer.

[24] Li, B. and Lima, D., 2021. Facial expression recognition via ResNet-50. International Journal of Cognitive Computing in Engineering, 2, pp.57-64.